



# Symmetry-Directed Self-Assembly of a Tetrahedral Protein Cage Mediated by de Novo-Designed Coiled Coils

Somayesadat Badieyan<sup>+, [a]</sup> Aaron Sciore<sup>+, [a]</sup> Joseph D. Eschweiler,<sup>[a]</sup> Philipp Koldewey,<sup>[b]</sup> Ajitha S. Cristie-David,<sup>[a]</sup> Brandon T. Ruotolo,<sup>[a]</sup> James C. A. Bardwell,<sup>[b, c, d]</sup> Min Su,<sup>[e]</sup> and E. Neil G. Marsh<sup>\*[a, c]</sup>

The organization of proteins into new hierarchical forms is an important challenge in synthetic biology. However, engineering new interactions between protein subunits is technically challenging and typically requires extensive redesign of protein–protein interfaces. We have developed a conceptually simple approach, based on symmetry principles, that uses short coiled-coil domains to assemble proteins into higher-order structures. Here, we demonstrate the assembly of a trimeric enzyme into a well-defined tetrahedral cage. This was achieved by genetically fusing a trimeric coiled-coil domain to its C terminus through a flexible polyglycine linker sequence. The linker length and coiled-coil strength were the only parameters that needed to be optimized to obtain a high yield of correctly assembled protein cages.

The assembly of protein subunits into higher-order structures is ubiquitous in nature and often appears to be guided by the principles of symmetry.<sup>[1]</sup> These natural protein assemblies have inspired the fields of synthetic biology and nanotechnology to apply symmetry principles to the design of new self-assembling protein systems. Among the architectures that have been achieved are: 1D protein fibers and rings; 2D and 3D protein lattices; and tetrahedral, octahedral, and icosahedral protein cages.<sup>[2]</sup>

The principle challenge to designing protein cages and lattices with well-defined architectures lies in precisely aligning the

two rotational symmetry axes at the correct angle necessary to specify the intended geometry.<sup>[3]</sup> One approach involves engineering new  $C_2$ -symmetric interfaces into oligomeric proteins, generally  $C_3$ -symmetric trimers, to provide the second symmetry axis needed to mediate assembly. The rigid interface ensures that the  $C_2$  and  $C_3$  symmetry axes are aligned with the precision necessary to specify the desired geometry. However, this approach requires extensive computational resources to evaluate candidate designs in silico and screening of many trial designs to identify successful assemblies. The extensive mutations introduced to create the new protein–protein interface might also compromise the protein's biological activity.

We have focused on an alternative approach to protein assembly that uses a flexible linker sequence to connect the two symmetry elements, for example, by fusing a  $C_2$  dimeric protein to a  $C_3$  trimeric protein.<sup>[4]</sup> Normally, this results in polydisperse assemblies, due to the limited control over the orientation of the two domains. However, we recognized that using protein elements with rotational symmetries of  $C_3$  or higher significantly restricts the number of compatible geometries so that unique structures can, in principle, form. Relaxing the requirement that the rotational symmetry axes need to be rigidly aligned greatly simplifies the design process.

Coiled-coil proteins are attractive components for this flexible approach as they are among the simplest and best-understood protein–protein interactions. There are a large number of well-characterized, de-novo-designed coiled coils available as “off-the-shelf” components that can be fused to larger natural protein subunits to mediate assembly.<sup>[5]</sup> This design strategy naturally lends itself to a modular approach for constructing protein cages: by mixing and matching protein building blocks and coiled-coil domains with different rotational symmetries, it should be possible to assemble protein cages with different geometries (Figure 1).

Previously,<sup>[4a]</sup> we selected a trimeric esterase (PDB ID: 1ZOI)<sup>[6]</sup> as a  $C_3$ -symmetric protein building block for the assembly of an octahedral cage assembled with a tetrameric coiled coil. This protein was chosen because each subunit comprises a single domain, and the C terminus is located near the apex of the triangle formed by the three subunits; this should minimize possible steric interference associated with assembling the trimeric subunits around the coiled-coil domain. Other than these, no other structural criteria were applied in the selection of the protein.

In this study, we aimed to investigate whether the octahedral cage could be converted to a tetrahedral cage by replac-

[a] Dr. S. Badieyan,<sup>+</sup> Dr. A. Sciore,<sup>+</sup> Dr. J. D. Eschweiler, A. S. Cristie-David, Prof. B. T. Ruotolo, Prof. E. N. G. Marsh  
Department of Chemistry, University of Michigan  
Ann Arbor, MI 48109 (USA)  
E-mail: nmarsh@umich.edu

[b] Dr. P. Koldewey, Prof. J. C. A. Bardwell  
Department of Molecular  
Cellular and Developmental Biology, University of Michigan  
Ann Arbor, MI 48109 (USA)

[c] Prof. J. C. A. Bardwell, Prof. E. N. G. Marsh  
Department of Biological Chemistry, University of Michigan  
Ann Arbor, MI 48109 (USA)

[d] Prof. J. C. A. Bardwell  
Howard Hughes Medical Institute, University of Michigan  
Ann Arbor, MI 40109 (USA)

[e] Dr. M. Su  
Life Sciences Institute, University of Michigan  
Ann Arbor, MI 48109 (USA)

[\*] These authors contributed equally to this work.

Supporting information and the ORCID identification numbers for the authors of this article can be found under <https://doi.org/10.1002/cbic.201700406>.

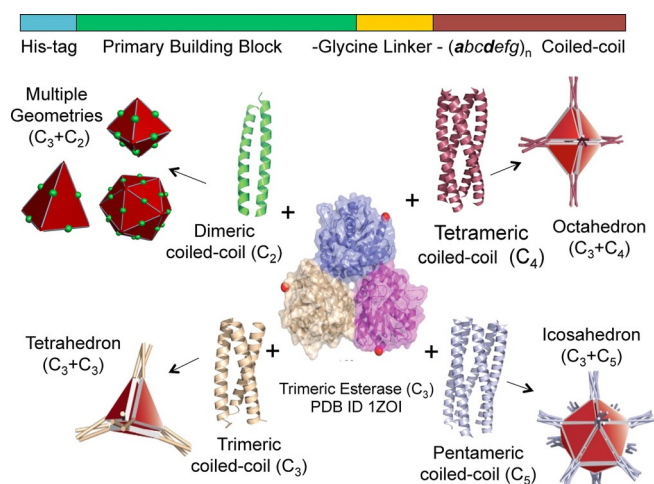


**Figure 1.** Design scheme: By fusing the C terminus (●) of a trimeric protein through a flexible linker to coiled coils with different oligomerization states, protein cages of different geometries can be assembled. The geometry is specified by the combination of symmetry axes.

ing the  $C_4$  symmetric four-stranded coiled-coil domain with a  $C_3$ -symmetric three-stranded coiled coil. We selected a crystallographically characterized, de-novo-designed trimeric, parallel coiled coil (PDB ID: 4DZL)<sup>[5]</sup> for this purpose. This coiled coil comprised four repeating heptads of sequence IAAIKQE, with the trimer structure being principally maintained by Ile residues at the hydrophobic a and d positions.<sup>[5]</sup>

To estimate the minimal length of linker needed to connect the C terminus of the esterase to the N terminus of the coiled coil, the  $C_3$  axes of the esterase and coiled coil were computationally aligned along the  $C_3$  axes defining the tetrahedral point group. By using an algorithm implemented in Rosetta,<sup>[7]</sup> the distance from the origin of each protein and its angle of rotation about its symmetry axis were allowed to vary whilst maintaining tetrahedral symmetry (Figure S1 in the Supporting Information).<sup>[4a]</sup> Configurations with inter-subunit backbone atom distances shorter than 4 Å, representing steric clashes, were discarded. In this manner, the minimum distance between the N and C termini was estimated as  $\approx 12$  Å, a distance that could be spanned by a four-residue glycine linker.

Based on our model, a gene encoding a fusion protein in which the C terminus of the esterase was linked to the N terminus of the trimeric coiled-coil domain through a Gly<sub>4</sub> linker sequence was assembled by standard methods (Figure S2). This protein, designated Tet4, was overexpressed in *Escherichia coli* BL21 and purified to homogeneity by using an N-terminal His-tag. Tet4 expressed as a soluble protein; however, initial analysis by native PAGE and size-exclusion chromatography (SEC) indicated that it formed an ensemble of oligomeric species with  $M_r > 600$  kDa (Figure 2), significantly larger than the  $M_r$  of  $\approx 430$  kDa expected for a tetrahedral cage.

As it seemed that a Gly<sub>4</sub> linker might be too short to allow the correct protein–protein interactions to form, we increased the length of the linker to six and eight glycine residues to give constructs Tet6 and Tet8. Analysis by SEC and native PAGE indicated that a complex of the correct molecular weight was

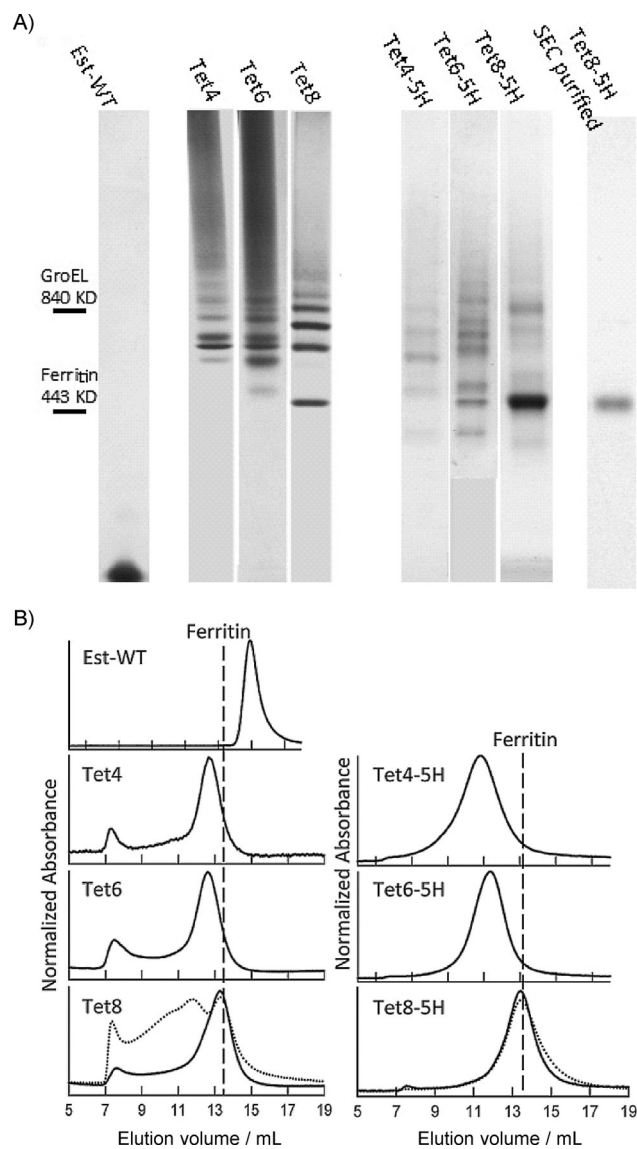


**Figure 2.** Screening Tet constructs with different linker lengths and coiled-coil strengths for their ability to assemble into cages. A) Characterization by native PAGE (migration of standard proteins indicated on left; Est-WT: parent esterase); B) SEC of Tet constructs. Dotted traces represent the elution profiles of Tet8 and Tet8-5H after storage for 4 months at 4 °C.

formed by Tet8. SEC-purified Tet8 was further analyzed by negative-stain electron microscopy (EM) and native mass spectrometry (native MS), which indicated that complexes of the expected morphology and molecular weight were being formed (Figure S3). However, the yield of correctly assembled protein cages was only  $\approx 25\%$ , as judged by native PAGE, and further variation of the linker length provided no additional selectivity for tetrahedral complexes.

To optimize the design, we investigated the effect of strengthening the coiled-coil interaction by increasing the number of IAAIKQE heptad repeats from four to five. We synthesized constructs in which the trimeric esterase was fused to the five-heptad coiled coil through a four-, six-, eight- or ten-residue glycine linker (referred to as Tet4-5H, Tet6-5H, Tet8-5H, and Tet10-5H, respectively). Analysis of the Tet4-5H and Tet6-

5H constructs by native PAGE indicated that they formed a mixture of oligomerization states with a similar size distribution to Tet4 and Tet6. However, Tet8-5H was far more homogeneous (Figure 2). It primarily comprised one oligomerization state after nickel-affinity chromatography and could be obtained in high yields of 10–20 mg purified protein per liter of culture. Further purification by SEC yielded material with the approximate  $M_r$  expected for a tetrahedron that was nearly homogeneous, as judged by native PAGE (Figure 2). Surprisingly, whereas Tet4-5H, Tet6-5H, and Tet8-5H were stable for months at 4 °C, Tet10-5H spontaneously formed insoluble aggregates in a matter of days.

Based on the promising characteristics of Tet8-5H, its structure was further analyzed by analytical ultracentrifugation (AUC), native MS, negative stain EM and cryo-EM. Sedimentation velocity AUC of Tet8-5H was performed at 122434  $g$ , and the sedimentation traces were subjected to 2D sedimentation spectrum analysis<sup>[8]</sup> (2DSA) to fit the velocity traces to the Lamm equation. This technique determines the sedimentation coefficient ( $s$ ) and frictional ratio ( $f/f_0$ ) of sedimenting species. The 2DSA plot of Tet8-5H (Figure 3A) shows a single hydrodynamic species with  $s_{20,w} = 14$  S and  $f/f_0 = 1.5$  (Table S1). The frictional ratio is within the range measured for proteins such as ferritin ( $f/f_0 = 1.3$ )<sup>[9]</sup> and the E2 complex of pyruvate dehydrogenase ( $f/f_0 = 2.5$ ), which also adopt porous cage-like struc-

tures.<sup>[10]</sup> The  $M_r$  of Tet8-5H calculated from these data was 430 kDa, closely matching the expected molecular weight of 439 kDa for a tetrahedral assembly comprising 12 protein subunits.

As a complementary technique to determine the oligomerization state of Tet8-5H, we examined its structure by native ESI MS.<sup>[11]</sup> This technique uses very mild ionization and desolvation conditions that preserve noncovalent protein–protein interactions in the gas phase, thereby allowing subunit composition to be determined. The native MS spectrum of Tet8-5H (Figure 3B) exhibited an envelope of well-resolved peaks, with  $m/z$  ranging from 8000 to 10000. Deconvolution of this spectrum gave a mass of  $434 \pm 0.2$  kDa for Tet8-5H, in good agreement the 12-subunit assembly expected for a tetrahedron.

Negative stain EM of Tet8-5H clearly showed particles with the threefold symmetry characteristic of a tetrahedral structure (Figure 3C), although many of the particles had collapsed and splayed out in the carbon support during sample preparation. Initial cryo-EM images indicated that freezing disrupted the particles, a common problem with cryo-EM sample preparation.<sup>[12]</sup> Thus, samples of Tet8-5H were first reacted with a lysine-specific crosslinking agent to rigidify the particles (Figures 3D and S4). The crosslinked Tet8-5H particles were flash frozen and visualized by cryo-EM. Particles were selected automatically and subjected to reference-free alignment and clas-

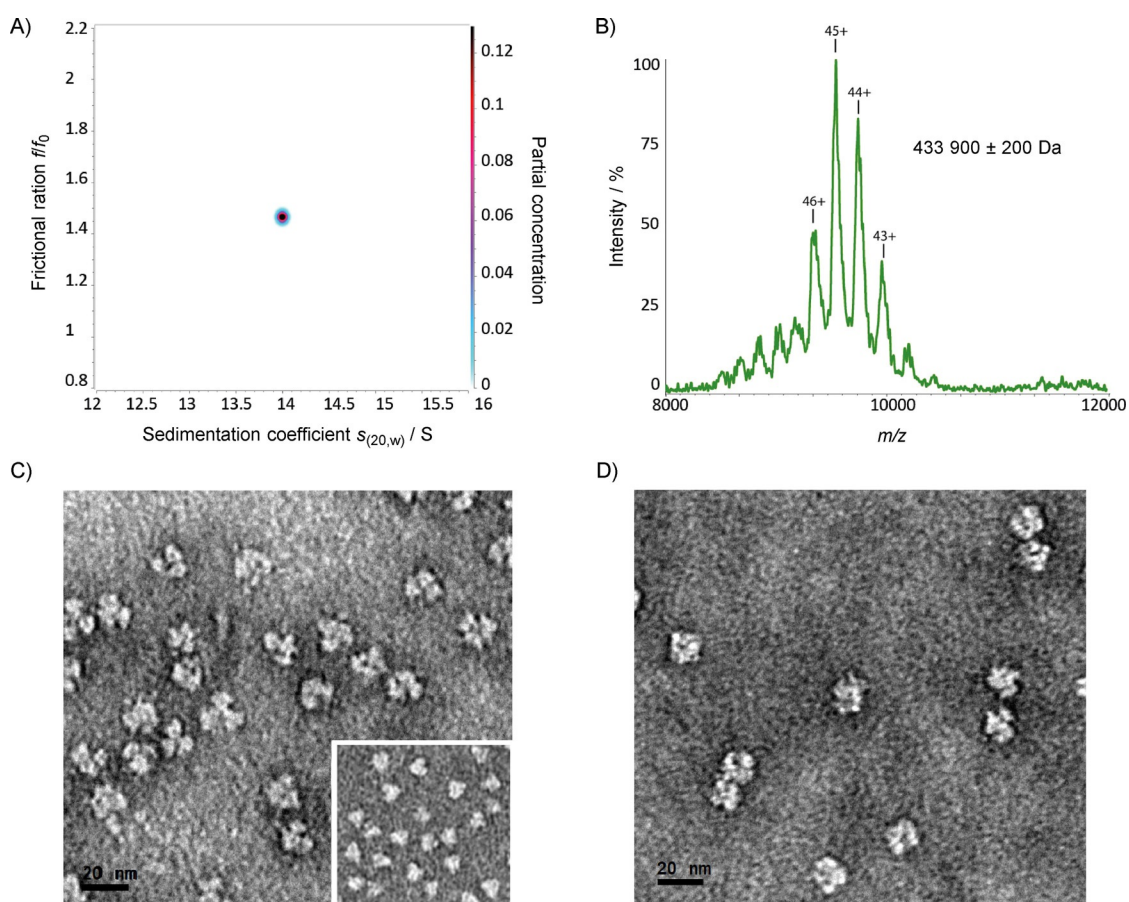


**Figure 3.** Characterization of Tet8-5H. A) Analytical ultracentrifugation; B) native MS; C) negative stain EM of Tet8-5H before and D) after crosslinking. Inset: TEM of wild-type trimeric esterase.



sification.<sup>[13]</sup> The 2D class averages revealed a variety of distinct views with well-resolved structural features (Figure S5). Many class averages showed thin projections emanating from the tetrahedral core that could be ascribed to the coiled-coil domains.

A total of 35 217 particles, extracted from fully assembled and well-defined class average images, were used to reconstruct a 3D model of Tet8-5H (Supporting Information). The final model, constrained by tetrahedral symmetry, had an indicated resolution of  $\approx 13$  Å (Figure S6). The map clearly revealed the arrangement of trimeric esterase domains and peripheral electron density attributable to the coiled-coil domains. The crystal structures of the trimeric esterase and the de-novo-designed trimeric coiled coil could be modeled into the electron density map, as shown in Figure 4. The resolution of the map did not allow us to unambiguously determine which face of the trimer faced outwards. The correlation coefficients between simulated map and EM density map, determined by using the Chimera "fit in map" tool, yield essentially the same value (0.6355 for the current docking and 0.6346 for the alternative face docking). However, in one orientation, the His<sub>6</sub>-tag used to purify the protein was sequestered within the cage,

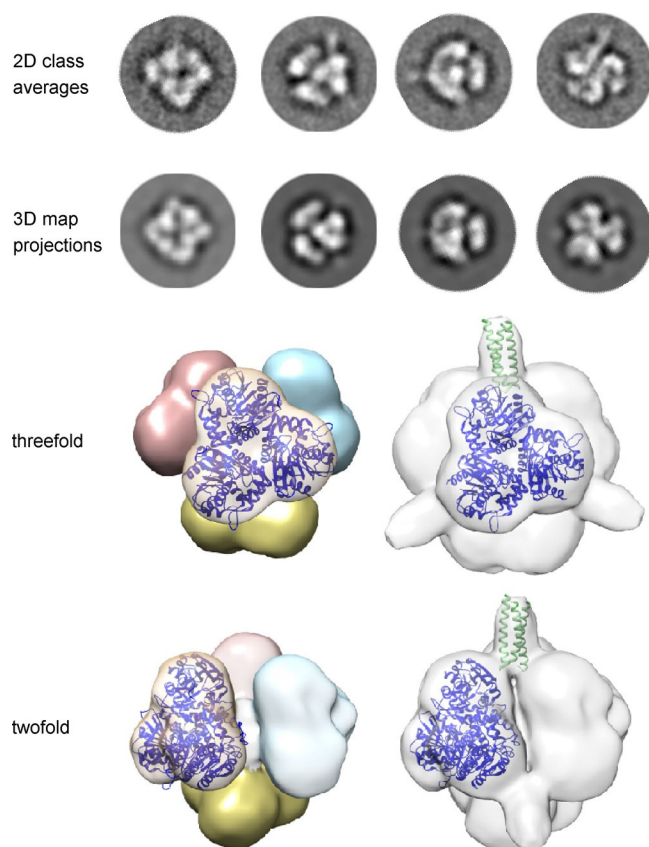


**Figure 4.** Top: Representative 2D class-averaged images of Tet8-5H and projections generated from the 3D electron density map. Bottom: Reconstructed electron density for Tet8-5H viewed along the threefold and twofold axes with one esterase trimer modeled into the electron density. At a lower threshold (gray), the 3D density map shows density for the coiled coils, allowing them to be docked into the map.

whereas in the other it pointed outward. Given that the protein bound tightly to the Ni-NTA column used to purify it, we consider the latter orientation to be more likely, and this determined our choice of model.

With the structures modeled into the electron density, the distance between the C terminus of the esterase and N terminus of the coiled coil was  $\approx 25$  Å (This distance was similar with the trimer docked in either orientation). This distance was slightly longer than could be spanned by the eight-glycine linker sequence, but given the resolution of the model and possible structural reorganization of the terminal residue, the modeled geometry appeared reasonable.

The esterase activity of purified Tet8-5H, with *p*-nitrophenol acetate as substrate, was found to be very similar to the parent esterase enzyme, and both the parent esterase and Tet8-5H showed similar thermal stability profiles, with  $T_m \approx 78$  °C (Figures S7 and S8). These observations indicated that the structure of the trimeric esterase was not significantly perturbed by the addition of the coiled-coil domain and subsequent assembly of the protein into a cage.

Our results demonstrate that it is possible to apply the principles of symmetry to direct the assembly of a generic trimeric protein into large-scale geometrical structures without explicitly specifying the orientation between symmetry axes. Thus, the same protein can be assembled into either octahedral or tetrahedral cages, depending simply on the choice of the coiled-coil domain. These results provide a striking demonstration of the utility of coiled coils as modular components for protein assembly.

To achieve the desired tetrahedral assembly, it was necessary to optimize both the glycine linker length and the coiled-coil strength. In particular, whereas a four-heptad coiled coil was satisfactory for assembling an octahedral cage,<sup>[4a]</sup> a five-heptad coiled coil was needed to achieve good yields of the tetrahedral cage. This might reflect the smaller hydrophobic core associated with the trimeric, as opposed to the tetrameric, coiled-coil design.

Also noteworthy is the sensitivity of the assembly process to glycine linker length. In this case, a Gly<sub>8</sub> linker gave a much more homogenous preparation than a Gly<sub>6</sub> or Gly<sub>4</sub> linker, whereas a Gly<sub>10</sub> linker resulted in an assembly that was unstable and prone to aggregation. The factors that determine the optimal linker length remain poorly understood. Presumably, a linker that is too short results in unfavorable steric interactions between the large esterase domains, preventing the protein from assembling as intended, whereas an overly long linker might allow coiled coils attached to esterase subunits in the same trimer to self-associate.

These results suggest that other trimeric proteins could be assembled into octahedral and tetrahedral cages by selecting the appropriate coiled coil and sampling a fairly sparse matrix of coiled-coil and linker lengths to optimize the assembly process. Furthermore, this approach could be extended to assemble proteins into a wider range of geometrical structures by selecting protein building blocks and coiled coils with different combinations of rotational symmetries. For example, by combining  $C_4$  and  $C_5$  systemic proteins with trimeric coiled coils,

cubic and dodecahedral constructs could, in principle, be formed.

## Acknowledgements

This work was supported by grants from the Army Research Office (W911NF-11-1-0251 and W911NF-16-1-0147 to E.N.G.M.). J.C.A.B. acknowledges support from the Howard Hughes Foundation. Supercomputer resources at the Texas Advanced Computing Center and the San Diego Supercomputer Center were used to analyze AUC data.

## Conflict of Interest

The authors declare no conflict of interest.

**Keywords:** coiled coils · protein cages · protein design · self-assembly · symmetry

- [1] a) T. O. Yeates, M. C. Thompson, T. A. Bobik, *Curr. Opin. Struct. Biol.* **2011**, *21*, 223–231; b) J. A. Marsh, S. A. Teichmann, *Annu. Rev. Biochem.* **2015**, *84*, 551–575.
- [2] a) J. B. Bale, S. Gonen, Y. Liu, W. Sheffler, D. Ellis, C. Thomas, D. Cascio, T. O. Yeates, T. Gonen, N. P. King, D. Baker, *Science* **2016**, *353*, 389–394; b) Y. Hsia, J. B. Bale, S. Gonen, D. Shi, W. Sheffler, K. K. Fong, U. Nattermann, C. Xu, P. S. Huang, R. Ravichandran, S. Yi, T. N. Davis, T. Gonen, N. P. King, D. Baker, *Nature* **2016**, *535*, 136–139; c) Y. T. Lai, G. L. Hura, K. N. Dyer, H. Y. Tang, J. A. Tainer, T. O. Yeates, *Science Adv.* **2016**, *2*, e1501855; d) T. O. Yeates, Y. Liu, J. Laniado, *Curr. Opin. Struct. Biol.* **2016**, *39*, 134–143; e) J. D. Brodin, X. I. Ambroggio, C. Tang, K. N. Parent, T. S. Baker, F. A. Tezcan, *Nat. Chem.* **2012**, *4*, 375–382; f) J. D. Brodin, S. J. Smith, J. R. Carr, F. A. Tezcan, *J. Am. Chem. Soc.* **2015**, *137*, 10468–10471.
- [3] a) P. S. Huang, S. E. Boyken, D. Baker, *Nature* **2016**, *537*, 320–327; b) C. H. Norn, I. Andre, *Curr. Opin. Struct. Biol.* **2016**, *39*, 39–45; c) Y. T. Lai, E. Reading, G. L. Hura, K. L. Tsai, A. Laganowsky, F. J. Asturias, J. A. Tainer, C. V. Robinson, T. O. Yeates, *Nat. Chem.* **2014**, *6*, 1065–1071.
- [4] a) A. Sciore, M. Su, P. Koldewey, J. D. Eschweiler, K. A. Diffley, B. M. Linhares, B. T. Ruotolo, J. C. Bardwell, G. Skiniotis, E. N. G. Marsh, *Proc. Natl. Acad. Sci. USA* **2016**, *113*, 8681–8686; b) D. P. Patterson, M. Su, T. M. Franzmann, A. Sciore, G. Skiniotis, E. N. G. Marsh, *Protein Sci.* **2014**, *23*, 190–199; c) D. P. Patterson, A. M. Desai, M. M. B. Holl, E. N. G. Marsh, *RSC Adv.* **2011**, *1*, 1004–1012; d) A. S. Cristie-David, A. Sciore, S. Badiyan, J. D. Eschweiler, P. Koldewey, B. T. Ruotolo, J. C. A. Bardwell, E. N. G. Marsh, *Mol. Syst. Design Engin.* **2017**, *2*, 140–148; e) F. B. L. Coughon, *ChemBioChem* **2016**, *17*, 2296–2298.
- [5] J. M. Fletcher, A. L. Boyle, M. Bruning, G. J. Bartlett, T. L. Vincent, N. R. Zaccai, C. T. Armstrong, E. H. C. Bromley, P. J. Booth, R. L. Brady, A. R. Thomson, D. N. Woolfson, *ACS Synth. Biol.* **2012**, *1*, 240–250.
- [6] F. Elmi, H. T. Lee, J. Y. Huang, Y. C. Hsieh, Y. L. Wang, Y. J. Chen, S. Y. Shaw, C. J. Chen, *J. Bacteriol.* **2005**, *187*, 8470–8476.
- [7] R. Das, D. Baker, *Annu. Rev. Biochem.* **2008**, *77*, 363–382.
- [8] a) B. Demeler, H. Saber, J. C. Hansen, *Biophys. J.* **1997**, *72*, 397–407; b) B. Demeler, K. E. van Holde, *Anal. Biochem.* **2004**, *335*, 279–288.
- [9] G. Jutz, P. van Rijn, B. S. Miranda, A. Boeker, *Chem. Rev.* **2015**, *115*, 1653–1701.
- [10] H. J. Bosma, A. Dekok, B. W. Vanmarkwijk, C. Veeger, *Eur. J. Biochem.* **1984**, *140*, 273–280.
- [11] B. T. Ruotolo, J. L. Benesch, A. M. Sandercock, S. J. Hyung, C. V. Robinson, *Nat. Protoc.* **2008**, *3*, 1139–1152.
- [12] R. F. Thompson, M. Walker, C. A. Siebert, S. P. Muench, N. A. Ranson, *Methods* **2016**, *100*, 3–15.
- [13] S. H. Scheres, *J. Struct. Biol.* **2012**, *180*, 519–530.

Manuscript received: July 31, 2017

Accepted manuscript online: August 1, 2017

Version of record online: August 29, 2017